HHS Public Access

Author manuscript

Cell Biochem Biophys. Author manuscript; available in PMC 2018 June 01.

Published in final edited form as:

Cell Biochem Biophys. 2017 June ; 75(2): 247–253. doi:10.1007/s12013-016-0733-x.

Concurrent longitudinal EPR monitoring of tissue oxygenation, acidosis and reducing capacity in a mouse xenograft tumor models

Andrey A. Bobko[a,b], **Jason Evans**[c], **Nicholas C. Denko**[c], and **Valery V. Khramtsov**[a,b]

[a]In Vivo Multifunctional Magnetic Resonance center, Robert C. Byrd Health Science Center, West Virginia University, Morgantown, WV 26506, United States

[b]Department of Biochemistry, West Virginia University School of Medicine, Morgantown, WV 26506, United States

[c]The James Comprehensive Cancer Center, The Ohio State University, Columbus, OH, United States

Abstract

Tissue oxygenation, extracellular acidity and tissue reducing capacity are among crucial parameters of tumor microenvironment (TME) of significant importance for tumor pathophysiology. In this paper we demonstrate the complementary application of particulate lithium octa-n-butoxy-naphthalocyanine (LiNc-BuO) and soluble nitroxide (NR) paramagnetic probes for monitoring of these TME parameters using electron paramagnetic resonance (EPR) technique. Two different types of therapeutic interventions were studied: hypothermia and systemic administration of metabolically active drug. *In summary*, the results demonstrate utility of EPR technique for noninvasive concurrent longitudinal monitoring of physiologically relevant chemical parameters of TME in a mouse xenograft tumor models including that under therapeutic intervention.

Introduction

Tumor tissue hypoxia is well documented[1] and is considered to be a consequence of imbalanced angiogenesis and is associated with changes in metabolism including higher dependence on glycolysis. Tissue hypoxia is associated with extracellular tissue acidosis due to Warburg effect[2] and poor tissue perfusion. Changes in cellular metabolism, tissue hypoxia and acidosis affect tissue redox status[3] [4]. Normalization of these parameters was found to be associated with inhibition of tumor grows and its metastatic activity correlating with efficiency of therapeutic intervention[5–11]. Therefore, noninvasive *in vivo* assessment of these parameters may provide important knowledge for advanced TME-targeted anticancer therapies[4, 12–14].

Correspondence to: Valery V. Khramtsov.

In this paper we demonstrate the complementary application of particulate (LiNc-BuO) and soluble (NR) paramagnetic probes for monitoring of basic TME parameters (oxygenation, pO_2; extracellular acidity, pH_e, and reducing capacity) using electron paramagnetic resonance (EPR) technique, including that under therapeutic intervention.

Lithium octa-n-butoxy-naphthalocyanine (LiNc-BuO) oximetric probe[15] (see Fig. 1 for the chemical structure) was successfully implemented for monitoring of pO_2 values in various biological systems. In particular, LiNc-BuO probe was applied for pO_2 detection in xenograft tumors when paramagnetic microcrystals were fully or partially internalized by cells and then delivered in tumor cell suspension. This approach is allowed for distribution and spreading of crystalline probes during tumor growth over whole tumor volume[15, 16]. The microcrystals are biologically inert probes which allows for repetitive detection of EPR signal during long period of time (up to 1 month). The EPR spectra of LiNc-BuO microcrystals is a single line (Fig 2.A.) of Lorentzian shape[17] with linewidth being sensitive to oxygen due to physical interaction between paramagnetic centers of crystal and oxygen diradical.

Analysis of Lorentzian linewidth of LiNc-BuO EPR spectra on oxygen concentration (see [17] and Materials and Methods Section) provides probe calibration parameters which than can be used in experiments for calculation of unknown pO_2 value.

Particulate probes are the probes of choice when measurement of pO_2 values is desired for long time and in predetermined area of interest. However particulate probe does not allow for detection of other physiologically relevant chemical parameters of TME beyond oxygen, and does not applicable for imaging studies. Therefore, soluble probes have advantage for imaging studies and detection multiple physiologically relevant TME parameters. Recently developed extracellular targeted dual function pH-sensitive nitroxide probe (NR, see Figure 1) represent useful soluble nontoxic probes for EPR-based imaging of pH_e and redox in vivo[8, 18, 19].

In this work we propose application of the nitroxide NR in combination with LiNc-BuO particulate probe for concurrent monitoring of TME oxygenation, acidosis and redox properties. Two different types of therapeutic interventions were studied: hypothermia and systemic administration of metabolically active drug, 1-(3,4-dimethoxybenzyl)-6,7-dimethoxyisoquinoline, DQ. Hypothermia was reported to improve oxygenation of tumors in normal or hyperbaric conditions [20–22]. DQ is a smooth-muscle relaxation agent [23] which was found to be oxygen consumption inhibitor in cell cultures[24] providing opportunity to alter the oxygenation of tumor tissue upon administration in vivo.

Materials and methods

Reagents

LiNc-BuO microcrystals were synthesized and prepared as described in [15, 25]. The synthesis of pH-sensitive nitroxide (NR) probes were performed as previously described in [8]. A smooth muscle relaxation drug, 1-(3,4-dimethoxybenzyl)-6,7-dimethoxyisoquinoline hydrochloride, abbreviated further as DQ, was purchased from Sigma-Aldrich.

Microcrystals oxygen sensitivity calibration

Microcrystals were dispersed in phosphate buffered saline (PBS, 1 mg/ml) in 1.5 ml centrifuge tube. Centrifuge tube was placed in surface coil resonator of EPR spectrometer and EPR spectra were acquired at different temperatures and oxygen concentrations. Temperature was controlled using water bath attached to the thermostat. To calibrate the sensitivity of microcrystals to oxygen partial pressure at given temperature, EPR spectra were recorded in air-bubbled and anoxic solutions. Anoxia in samples was maintained by using glucose/glucose oxidase enzymatic system [8]. EPR spectra were fitted with Lorentzian shape function to find line width, LW. The sensitivity of microcrystals to pO_2 was evaluated as a slope of the dependence of LW on pO_2, namely as a value (LW(air)-LW(anoxia))/pO_2(air), where LW(air) and LW(anoxia) are spectra linewidth in air and anoxia conditions, correspondingly; pO_2(air)=152 mmHg. In the temperature range from 26 °C to 33 °C oxygen sensitivity changed insignificantly being equal to 15.4 mG/mmHg at 26 °C, 13.7 mG/mmHg at 30 °C and 13.0 mG/mmHg at 33 °C, therefore average value of 14.0 mG/mmHg was used to calculate pO_2 values in following in vivo experiments. This temperature range was selected because the temperature of xerograph mouse tumor was in the range of 26–33 °C depending on heating condition and time of experiment. Nomad Fiber Optic Thermometer (Neoptix, Canada) equipped with Fiber Optic Temperature Sensor with a probe diameter of 0.5 mm and precision of ± 0.2°C was used to measure tumor temperature.

L-band (1.2 GHz) spectrometer (Magnettech, Bruker) acquisition parameters were as following: microwave power, 13 dB; modulation amplitude, 0.375 G; modulation frequency, 100 kHz; sweep width, 5 G; sweep time, 60 s.

Cell Culture

A549 human lung carcinoma cells and HCT 116 human colon carcinoma cells were maintained in Roswell Park Memorial Institute (RPMI) 1640 medium (Gibco) with 10% Fetal bovine serum, FBS, (Sigma) in a 5% CO_2 humidified atmosphere at 37°C.

Internalization of LiNc-BuO microcrystals into cells

A549 and HCT116 cells were plated at a density of 5×10^5 cells in 10cm cell culture dishes in 10mL RPMI 1640 media and were allowed to attach overnight. The next day media was replaced with 5ml fresh RPMI 1640 media. LiNc-BuO microcrystals were suspended in RPMI 1640 to a concentration of 20 mg/1ml and sonicated for 5 minutes on ice with a probe sonicator (Sonic Bismembrator, model 100; Fisher Scientific) at 20 kHz using 7 W power in a 5 mL glass round-bottom tube. 100 μl of this suspension was added to the cell culture dish containing the cells. Cells were incubated at 37°C for 72 hours or until they reached 80% confluency. Then cells were washed five times with PBS to remove non-internalized particles, trypsinized and 5×10^5 cells transferred to a new dish. Cells were allowed to attach for a minimum 4 hours and the cycle of particle addition and cell growth/particle internalization was repeated three more times (4 cycles total).

Animals and Tumor Xenografts

Nude mice were obtained from Charles River Laboratories at 8 weeks of age. Once the four cycles of LiNc-BuO microcrystals were complete, cells with the internalized particles were trypsinized, pelleted, and washed with Dulbecco's phosphate-buffered saline (1× dPBS, Gibco) three times. The cells were suspended at a concentration of 5×10^6 per 100 μl and placed on ice. Each mouse received one injection subcutaneously into the upper portion of the right hind limb of 5×10^6 cells (100 μl). Tumors appearance and growth was monitored every other day until they reached size 100 mm^3.

In Vivo L-Band EPR Studies

Mice were narcotized by inhalation of air-isoflurane mixture using Ohmeda Fluotec 3 anesthetic machine (2% isoflurane in 2 L/min O_2 flow) and then placed into the gap of L-band EPR spectrometer (Magnettech, Germany). The surface coil resonator was placed onto xenograft tumor and spectrometer was tuned. Experiment was performed on animals at ambient room temperature (23 °C) or using a thermopad (Pristech Products, Inc.) to maintain body temperature. Baseline measurements of the tumor were made for 5–10 minutes before drug administration. Saline (vehicle) and DQ (2 mg/kg dose in saline) were slowly administered via tail-vein injections at a total volume of 100μl. Once removed from anesthesia, mice were kept warm and monitored until they became ambulatory.

LiNc-BuO microcrystals experiments—EPR spectra of LiNc-BuO microcrystals embedded in to tumor tissue were measured using acquisition parameters listed in “Microcrystals oxygen sensitivity calibration” section for about 60 minutes. The pO_2 values were extracted from EPR line width using calibration data.

pH-sensitive nitroxide experiments—Experiments were performed according to published procedure [8]. The EPR spectra were acquired for about 3 min immediately after i.t. injection of the NR probe in saline solution (10 μL, 10 mM). The kinetics of left field component intensity and distance between low-field and high-field component of EPR spectra of the NR probe were measured to determine reduction rate constants and pH, correspondingly. The instrument settings were as follows: incident microwave power, 3 dB; modulation amplitude, 2.5 G; modulation frequency, 100 kHz; sweep width, 60 G; sweep time, 20 s.

Probes localization—Intratumoral localization of cell-embedded microcrystals and NR probe were previously supported by imaging studies reported in ref. [16] and [8] , correspondingly.

Results and Discussion

Application of LiNc-BuO microcrystals for longitudinal studies of tissue pO_2 dynamics

Fig. 2A shows typical in vivo EPR spectrum measured in vivo from A549 xenograft tumor in a nude mouse. The EPR signal arises from LiNc-BuO microcrystals internalized by the A549 human lung carcinoma cells used for initiation of tumor growth (see Materials and Methods). Spectrum demonstrates a single line of Lorentzian shape that allows for tissue

pO_2 calculation using calibration of microcrystal oxygen sensitivity. Fig. 2.B shows temporal dynamics of tissue pO_2 value in A549 xenograft tumor in a nude mouse during 60 minutes of anesthesia after i.v. injections of saline or DQ. In these experiments the anesthetized animals were not thermoregulated. It shows increase in tumor tissue oxygenation with time after injections of both DQ drug and saline solutions. Statistical analysis of these experiments is shown in Fig.3. It was found that pO_2 values at the beginning of experiment were lower and significantly different from pO_2 values at the end of experiment for both saline and drug injections. Note that similar results were obtained for relatively small and large tumors (compare statistics in Tables SI1 and SI2) and for different type of tumor cell lines (compare Tables SI1 and SI5 for tumor xenograft of A549 and HCCT116 cell lines). We hypothesized that the rise of pO_2 value over time of anesthesia might be related to low metabolic activity in anesthetized not thermoregulated (hypothermic) animals that results in slowing down the overall cellular oxygen consumption. This hypothesis was tested by using thermopad to maintain anesthetized animal body temperature during the experiment.

The results of these experiments are shown in Fig.4 and Table SI6. Indeed, thermoregulation of animals stabilized tissue oxygenation for entire duration (60 minutes) of the experiment. Note that effect of hypothermia on oxygen consumption and oxygen supply to tumors was previously described [21]. Authors showed that due to hypothermia oxygen consumption is decreased in tumor tissue while oxygen supply remain relatively constant. Therefore tissue thermoregulation might play a significant role in regulation of tissue oxygenation as demonstrated in our experiments (Fig.3 and Fig.4). Figure 4 also demonstrates that DQ does not affect tissue oxygenation. The absence of the effect of DQ might be explained by its inefficient delivery inside tumor cells in our experimental settings.

Application of soluble paramagnetic probes for studies of tumor tissue chemical microenvironment

In addition to tissue pO_2 measurements based on EPR signal of LiNc-BuO microcrystals embedded within tumor, we performed intratumoral (i.t.) nitroxide probe delivery for concurrent monitoring of TME acidosis and tissue reducing capacity. Figure 5A shows the EPR spectrum measured in vivo from A549 xenograft tumor in nude mouse after i.t. injection of soluble NR probe. The spectrum shows superposition of typical triplet spectral pattern of NR superimposed with a single EPR line of LiNc-BuO microcrystals embedded within tumor. Extracellular tissue acidity (pH_e) of tumor can be calculated from the distance between low-field (left) and high-field (right) components of NR spectra. Independently, tissue reducing capacity can be evaluated from the rate of the nitroxide EPR signal decay. Fig. 5B represents the kinetics of NR nitroxide low-field component decay measured before and 60 min after intravenous (i.v.) saline injections. Linear fitting of these kinetics allows for assessment of arbitrary value of tissue reducing capacity. Recently we have demonstrated [8] that tissue reducing capacity is a characteristic parameter that discriminate tumor tissue and normal mammary gland as well it is sensitive to therapeutic intervention. The EPR measurements performed in this work showed that 1 hour isoflurane anesthesia, hypothermia and DQ treatment did not affect reducing capacity of tumor tissue (Table SI4).

NR bifunctional probe allows for simultaneously detection of tissue reducing capacity and extracellular pH (pH_e). Fig.5C shows the measurement of pH in tumor tissue after probe injection before and 60 min after saline i.v. administration in mouse. We observed that 1 hour isoflurane anesthesia and hypothermia did not affect tumor tissue acidity, probably because of limited influence of anesthesia and hypothermia on tumor perfusion [21]. However we did observe significant acidification of tumor extracellular microenvironment after DQ treatment (see Fig.6). Note that DQ has a limited solubility at pH above 5 [26] and therefore is injected in acidic solution which apparently may result in acidification of extracellular tissue microenvironment.

In summary, the results demonstrate utility of EPR technique for noninvasive concurrent longitudinal monitoring of physiologically relevant chemical parameters of TME in a mouse xenograft tumor models including that under therapeutic intervention.

Supplementary Material

Refer to Web version on PubMed Central for supplementary material.

Acknowledgments

This work was partially supported by NIH grants CA194013, CA192064 and U54GM104942. The content is solely the responsibility of the authors and does not necessarily represent the official views of the NIH.

References

1. Tatum JL, Kelloff GJ, Gillies RJ, Arbeit JM, Brown JM, Chao KS, Chapman JD, Eckelman WC, Fyles AW, Giaccia AJ, Hill RP, Koch CJ, Krishna MC, Krohn KA, Lewis JS, Mason RP, Melillo G, Padhani AR, Powis G, Rajendran JG, Reba R, Robinson SP, Semenza GL, Swartz HM, Vaupel P, Yang D, Croft B, Hoffman J, Liu G, Stone H, Sullivan D. Hypoxia: importance in tumor biology, noninvasive measurement by imaging, and value of its measurement in the management of cancer therapy. Int J Radiat Biol. 2006; 82(10):699–757. [PubMed: 17118889]
2. Warburg O. On the origin of cancer cells. Science. 1956; 123(3191):309–314. [PubMed: 13298683]
3. Matsumoto K, Hyodo F, Matsumoto A, Koretsky AP, Sowers AL, Mitchell JB, Krishna MC. High-resolution mapping of tumor redox status by magnetic resonance imaging using nitroxides as redox-sensitive contrast agents. Clin Cancer Res. 2006; 12(8):2455–2462. [PubMed: 16638852]
4. Khramtsov VV, Gillies RJ. Janus-Faced Tumor Microenvironment and Redox. Antioxidants & Redox Signaling. 2014; 21(5):723–729. [PubMed: 24512276]
5. Bailey KM, Wojtkowiak JW, Cornnell HH, Ribeiro MC, Balagurunathan Y, Hashim AI, Gillies RJ. Mechanisms of buffer therapy resistance. Neoplasia (New York, N.Y.). 2014; 16(4):354.e3–364.e3.
6. Ribeiro, MdLC., Silva, AS., Bailey, KM., Kumar, NB., Sellers, TA., Gatenby, RA., Ibrahim-Hashim, A., Gillies, RJ. Buffer Therapy for Cancer. Journal of nutrition & food sciences. 2012; 2:6. [PubMed: 24371544]
7. Robey IF, Baggett BK, Kirkpatrick ND, Roe DJ, Dosescu J, Sloane BF, Hashim AI, Morse DL, Raghunand N, Gatenby RA, Gillies RJ. Bicarbonate Increases Tumor pH and Inhibits Spontaneous Metastases. Cancer research. 2009; 69(6):2260–2268. [PubMed: 19276390]
8. Bobko AA, Eubank TD, Voorhees JL, Efimova OV, Kirilyuk IA, Petryakov S, Trofimiov DG, Marsh CB, Zweier JL, Grigor'ev IA, Samouilov A, Khramtsov VV. In vivo monitoring of pH, redox status, and glutathione using L-band EPR for assessment of therapeutic effectiveness in solid tumors. Magn Reson Med. 2012; 67(6):1827–1836. [PubMed: 22113626]
9. Jain RK. Normalizing tumor microenvironment to treat cancer: bench to bedside to biomarkers. J Clin Oncol. 2013; 31(17):2205–2218. [PubMed: 23669226]

10. Fukumura D, Jain RK. Tumor microvasculature and microenvironment: Targets for anti-angiogenesis and normalization. Microvascular Research. 2007; 74(2–3):72–84. [PubMed: 17560615]
11. Denko NC. Hypoxic regulation of metabolism offers new opportunities for anticancer therapy. Expert review of anticancer therapy. 2014; 14(9):979–981. [PubMed: 24930453]
12. Roshchupkina GI, Bobko AA, Bratasz A, Reznikov VA, Kuppusamy P, Khramtsov VV. In vivo EPR measurement of glutathione in tumor-bearing mice using improved disulfide biradical probe. Free Radical Biology and Medicine. 2008; 45(3):312–320. [PubMed: 18468522]
13. Chen D, Bobko AA, Gross AC, Evans R, Marsh CB, Khramtsov VV, Eubank TD, Friedman A. Involvement of tumor macrophage HIFs in chemotherapy effectiveness: mathematical modeling of oxygen, pH, and glutathione. PLoS One. 2014; 9(10):e107511. [PubMed: 25295611]
14. Dhimitruka I, Bobko AA, Eubank TD, Komarov DA, Khramtsov VV. Phosphonated Trityl Probes for Concurrent in Vivo Tissue Oxygen and pH Monitoring Using Electron Paramagnetic Resonance-Based Techniques. Journal of the American Chemical Society. 2013; 135(15):5904–5910. [PubMed: 23517077]
15. Bratasz A, Pandian RP, Deng Y, Petryakov S, Grecula JC, Gupta N, Kuppusamy P. In Vivo Imaging of Changes in Tumor Oxygenation During Growth and After Treatment. Magnetic resonance in medicine : official journal of the Society of Magnetic Resonance in Medicine / Society of Magnetic Resonance in Medicine. 2007; 57(5):950–959.
16. Eubank TD, Roberts RD, Khan M, Curry JM, Nuovo GJ, Kuppusamy P, Marsh CB. GM-CSF INHIBITS BREAST CANCER GROWTH AND METASTASIS BY INVOKING AN ANTI-ANGIOGENIC PROGRAM IN TUMOR-EDUCATED MACROPHAGES. Cancer research. 2009; 69(5):2133–2140. [PubMed: 19223554]
17. Pandian RP, Dolgos M, Marginean C, Woodward PM, Hammel PC, Manoharan PT, Kuppusamy P. Molecular packing and magnetic properties of lithium naphthalocyanine crystals: hollow channels enabling permeability and paramagnetic sensitivity to molecular oxygen. Journal of materials chemistry. 2009; 19(24):4138–4147. [PubMed: 19809598]
18. Goodwin J, Yachi K, Nagane M, Yasui H, Miyake Y, Inanami O, Bobko AA, Khramtsov VV, Hirata H. In vivo tumour extracellular pH monitoring using electron paramagnetic resonance: the effect of X-ray irradiation. NMR in biomedicine. 2014; 27(4):453–458. [PubMed: 24470192]
19. Samouilov A, Efimova OV, Bobko AA, Sun Z, Petryakov S, Eubank TD, Trofimov DG, Kirilyuk IA, Grigor'ev IA, Takahashi W, Zweier JL, Khramtsov VV. In Vivo Proton–Electron Double-Resonance Imaging of Extracellular Tumor pH Using an Advanced Nitroxide Probe. Analytical Chemistry. 2014; 86(2):1045–1052. [PubMed: 24372284]
20. Nias AH, Perry P, Photiou A, Reghebi K. Effect of hypothermia on radiosensitization. Int J Radiat Biol Relat Stud Phys Chem Med. 1986; 50(2):241–251. [PubMed: 3488283]
21. Nias AH, Perry PM, Photiou AR. Modulating the oxygen tension in tumours by hypothermia and hyperbaric oxygen. Journal of the Royal Society of Medicine. 1988; 81(11):633–636. [PubMed: 3210193]
22. Sealy R, Harrison GG, Morrell D, Korrubel J, Gregory A, Barry L, Blekkenhorst G, Hering ER, Fataar AB, Boniaszczuk J. A feasibility study of a new approach to clinical radiosensitisation: hypothermia and hyperbaric oxygen in combination with pharmacological vasodilatation. Br J Radiol. 1986; 59(707):1093–1098. [PubMed: 3790896]
23. Evans GR, Gherardini G, Gurlek A, Langstein H, Joly GA, Cromeens DM, Sukumaran AV, Williams J, Kilbourn RG, Wang B, Lundeberg T. Drug-induced vasodilation in an in vitro and in vivo study: the effects of nicardipine, papaverine, and lidocaine on the rabbit carotid artery. Plast Reconstr Surg. 1997; 100(6):1475–1481. [PubMed: 9385959]
24. Shinozawa S, Araki Y, Oda T. Papaverine-induced changes in physiological characters of Ehrlich ascites tumor cell membranes. Physiol Chem Phys. 1980; 12(4):291–297. [PubMed: 7454853]
25. Pandian RP, Parinandi NL, Ilangovan G, Zweier JL, Kuppusamy P. Novel particulate spin probe for targeted determination of oxygen in cells and tissues. Free Radical Biology and Medicine. 2003; 35(9):1138–1148. [PubMed: 14572616]

26. Serajuddin AT, Rosoff M. pH-Solubility profile of papaverine hydrochloride and its relationship to the dissolution rate of sustained-release pellets. J Pharm Sci. 1984; 73(9):1203–1208. [PubMed: 6491936]

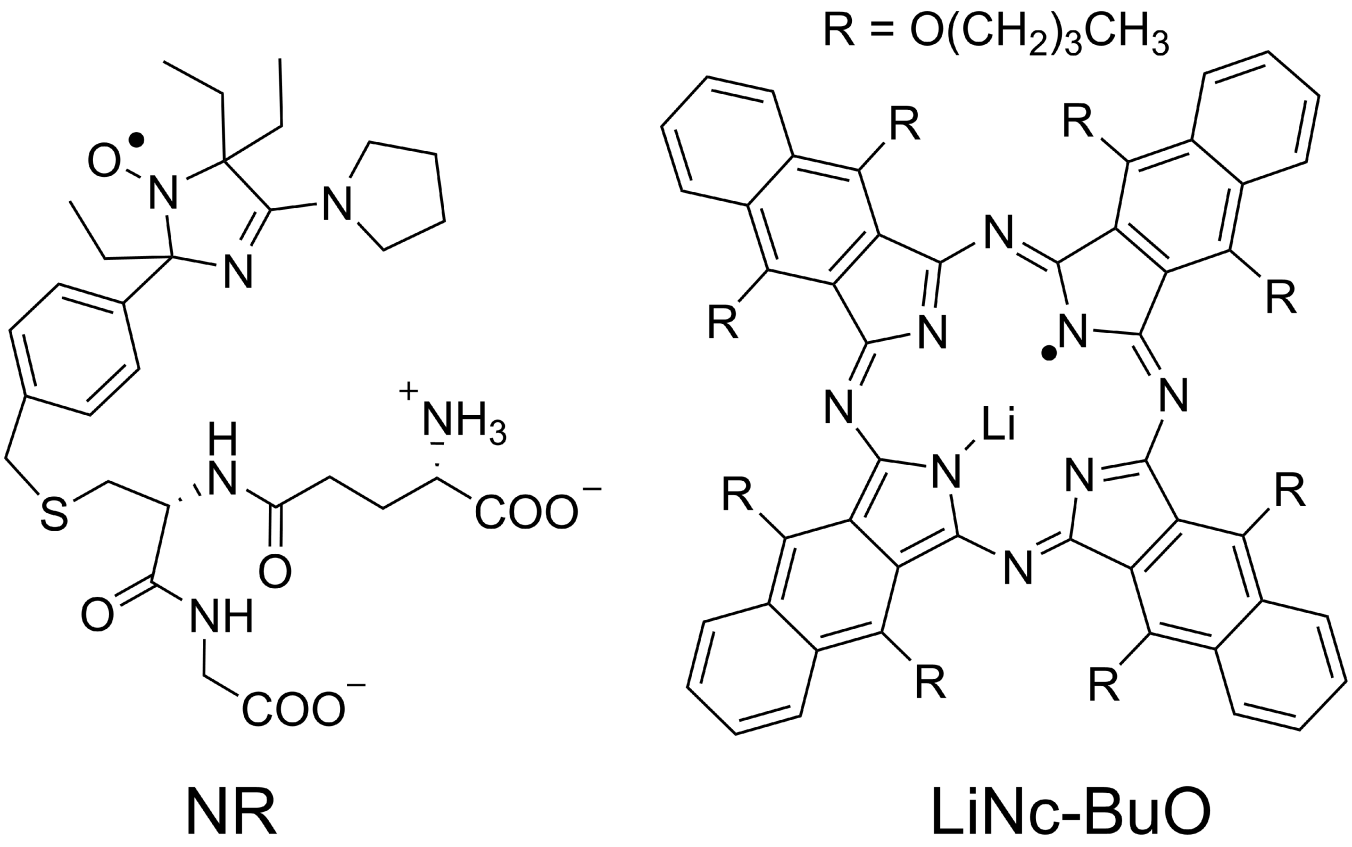

Figure 1.
Chemical structures of nitroxide soluble (NR; pH- and –redox sensitivity) and LiNc-BuO crystalline (pO_2 sensitivity) probes.

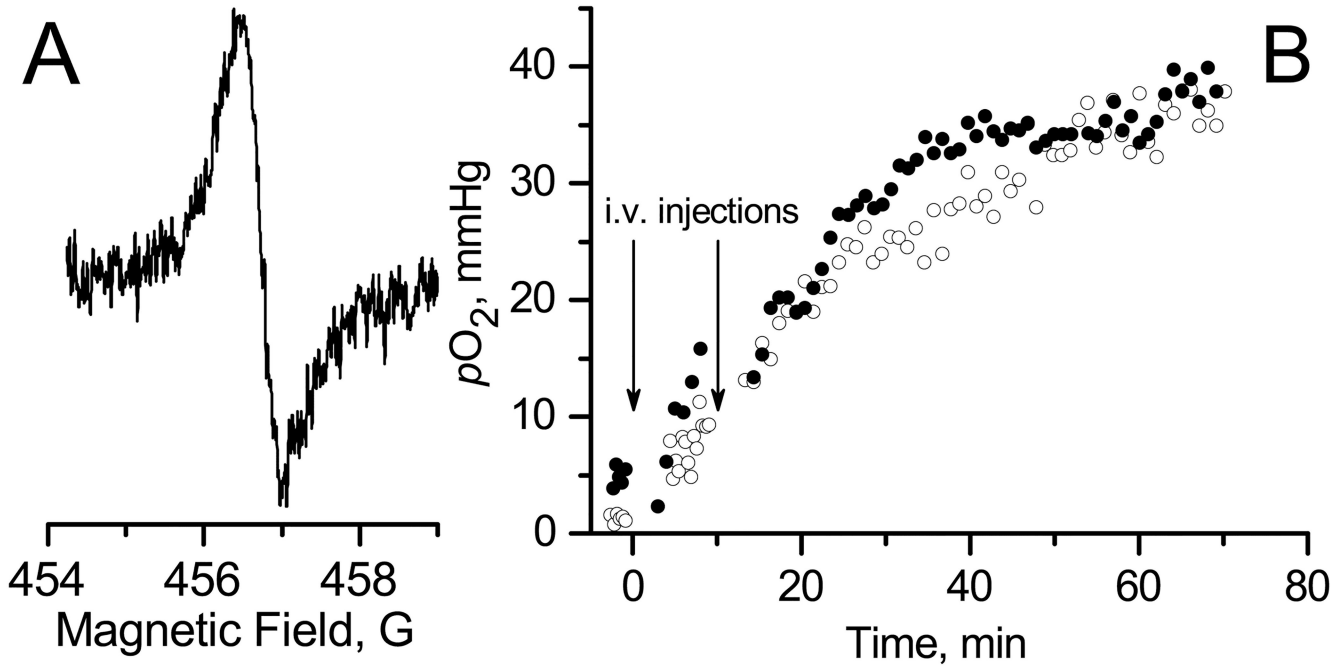

Figure 2.

A. EPR spectrum of LiNc-BuO microcrystals embedded into A549 xenograft tumor in nude mouse. ***B.*** The temporal dynamics of tumor tissue pO_2 values calculated from the width of EPR spectra (e.g. Fig.2.A.) measured in anesthetized mouse after two tail vein injection of control saline (○) or 2 mg/kg DQ drug (●) solution. Mice were not thermoregulated during EPR spectra acquisition.

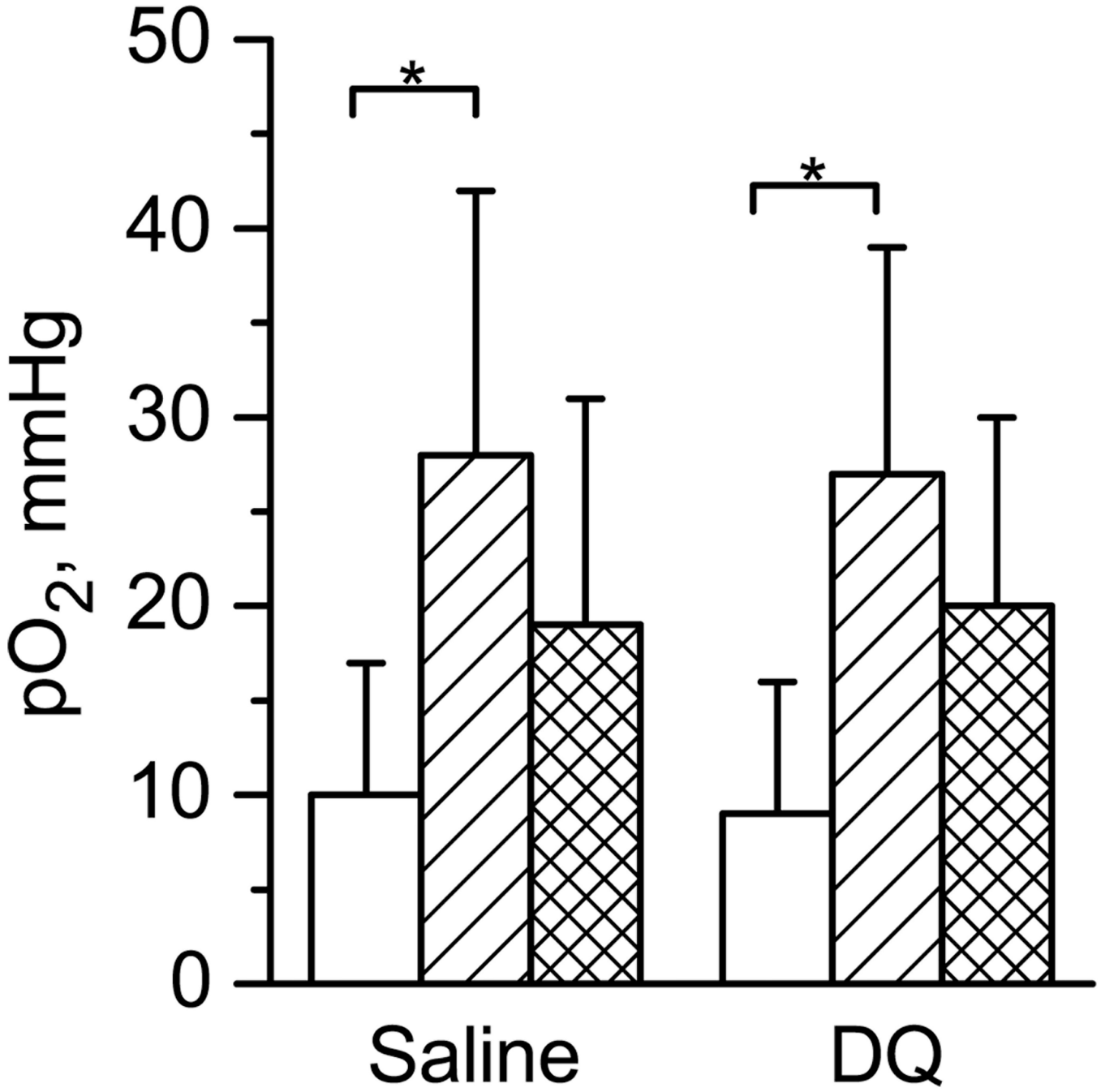

Figure 3.

The oxygenation of tumor tissue before (white columns) and after 60 min of saline or DQ tail vein injections (crossed columns). Double crossed columns shows the increase in tissue oxygenation. Animals were not thermoregulated. Number of animals was 9 and 5 for saline and DQ experiments, correspondingly. Average tumor volume was (45±20) μL and (46±21) μL for saline and DQ experiments, correspondingly. Errors are SD values. *p <0.007.

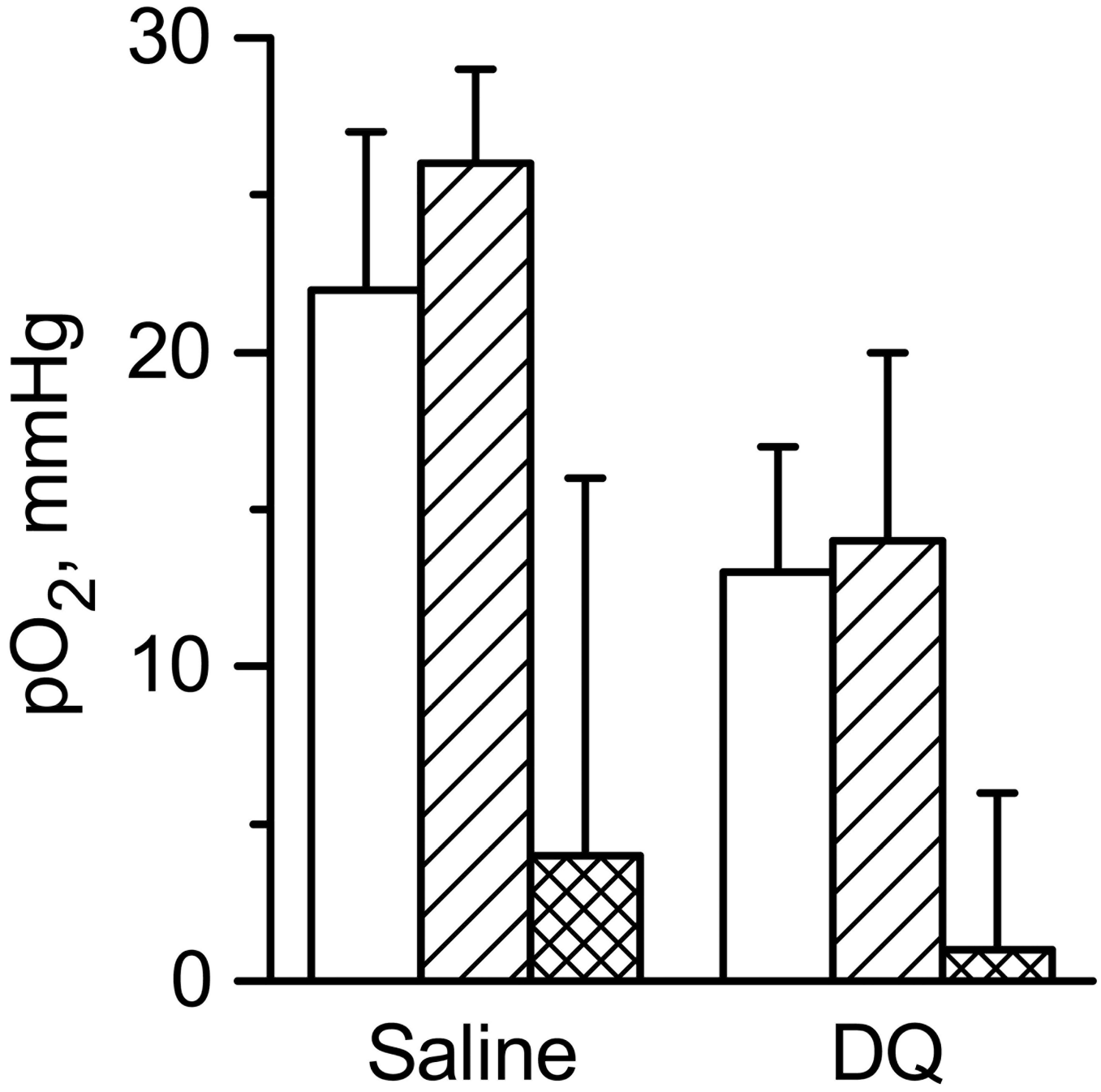

Figure 4.

The oxygenation of tumor tissue measured by LiNc-BuO microcrystals before (white columns) and after 60 min of saline or DQ tail vein injections (crossed columns). Double crossed columns shows the increase in tissue oxygenation. Animals were subject to thermoregulation protocol procedure using thermopad. Number of animals was 3 and 4 for saline and DQ experiments, correspondingly. Average tumor volume was (46±10) μL and (45±11) μL for saline and DQ injections experiments, correspondingly. Errors are SD values.

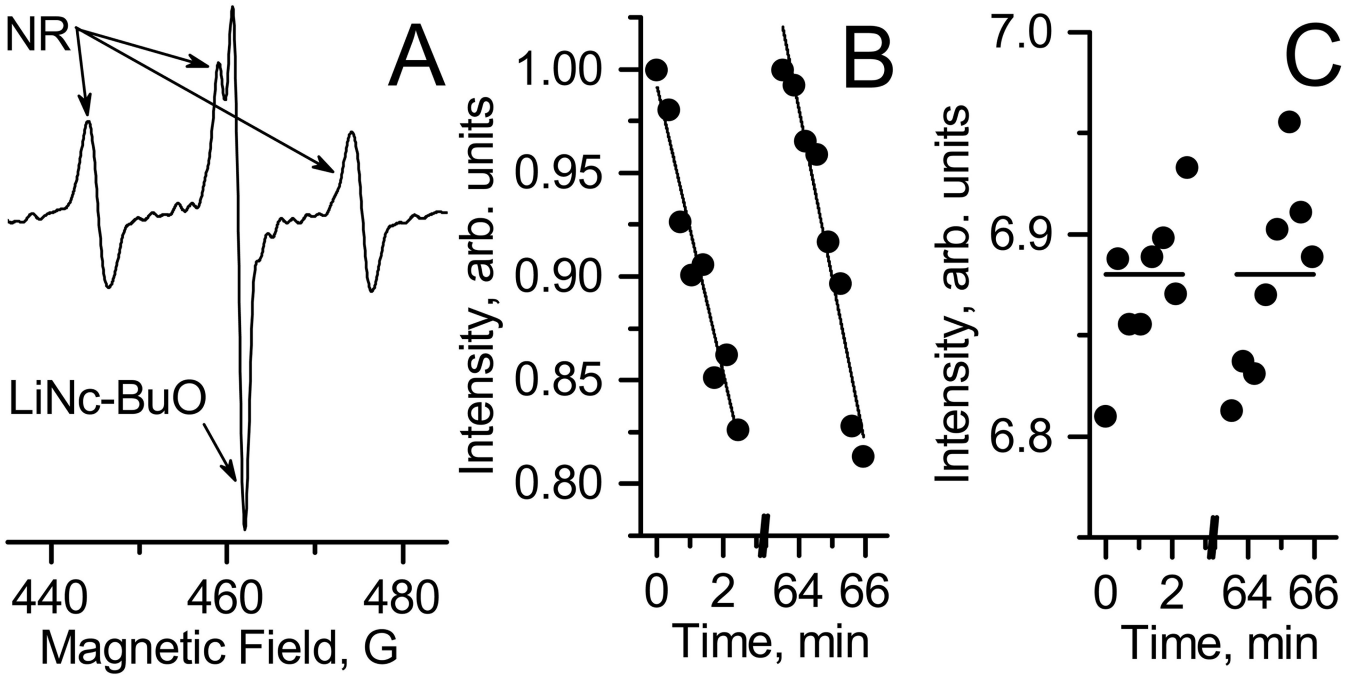

Figure 5.

A. EPR spectrum measured in vivo from A 549 xenograft tumor in nude mouse after i.t. injection of soluble NR probe. The observed triplet spectrum of the NR is superimposed with a single EPR line of LiNc-BuO microcrystals embedded within tumor. ***B.*** The normalized kinetics of low-filed component of NR EPR spectra before and 60 minutes after i.v. tail injection of saline solution. Lines represent the linear fittings of kinetics yielding values $1.15 \cdot 10^{-3}$ s^{-1} and $1.35 \cdot 10^{-3}$ s^{-1} for line slope for 1^{st} and 2^{nd} kinetics, correspondingly. ***C.*** pH values obtained using EPR spectra of NR probe before and 60 minutes after saline injections. Horizontal lines are represent the average values equal to 6.88.

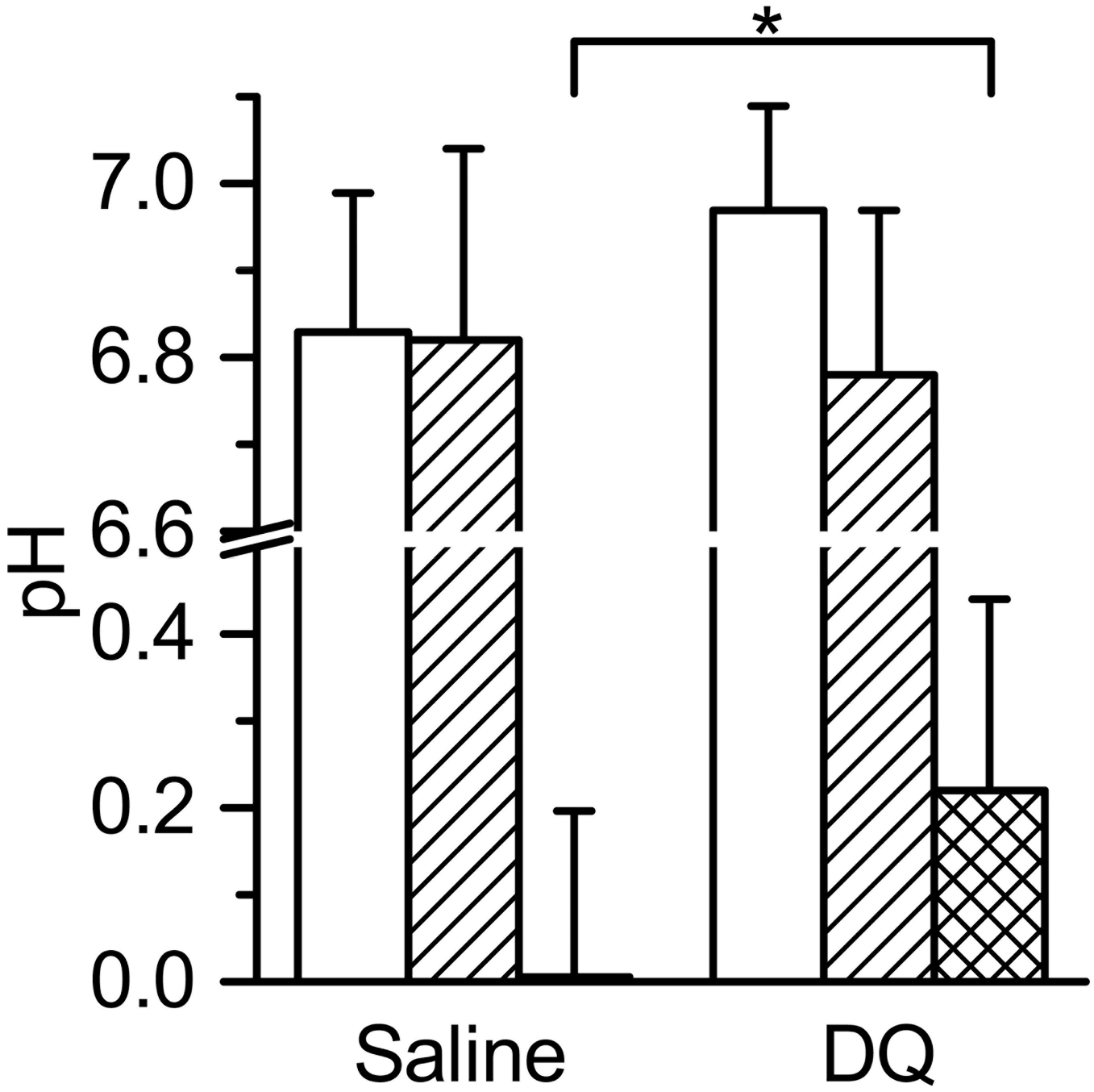

Figure 6.

The acidity values of tumor tissue measured by NR soluble probe before (white columns) and 60 min after saline or DQ i.v. tail vein injections (crossed columns). Double crossed columns shows the change in pH_e. Animals were not thermoregulated. Number of animals was 11 and 8 for saline and DQ experiments, correspondingly. Average tumor volume was (57±31) μL and (77±33) μL for saline and DQ experiments, correspondingly. Errors are SD values. *p <0.04.